(article starts on next page)

DNS of Dispersed Multiphase Flows with Heat Transfer and Rarefaction Effects

Henrik Ström and Srdjan Sasic

DNS of Dispersed Multiphase Flows with Heat Transfer and Rarefaction Effects

Henrik Ström* and Srdjan Sasic
Department of Applied Mechanics, Division of Fluid Dynamics,
Chalmers University of Technology, Gothenburg, Sweden

Abstract
We propose a method for DNS of particle motion in non-isothermal systems. The method uses a shared set of momentum and energy balance equations for the carrier- and the dispersed phases. Measures are taken to ensure that non-deformable entities (solid particles) behave like rigid bodies. Moreover, deformable entities (e.g. bubbles) as well as rarefaction effects can be accommodated. The predictions of the method agree well with the available data for isothermal solid particles motion in the presence of walls and other particles, natural convection around a stationary particle, solid particles motion accompanied with heat transfer effects and isothermal solid particles motion under rarefied conditions. The method is used to investigate the simultaneous effects of heat transfer and rarefaction on the motion of a solid catalyst particle in an enclosure, the interaction of a solid particle and a microbubble in a flotation cell and a case with more than 1000 particles.

1. INTRODUCTION

In a number of industrial applications, more than two types of dispersed phases co-exist and interact. Important examples include flotation (solid particles and bubbles in a liquid), and in-cylinder diesel spray combustion and spray drying with particle nucleation (droplets and solid particles in a gas). The transport of momentum and heat can be strongly coupled in these systems, so that the motion of the dispersed phases is significantly affected by the heat transfer and vice versa.

Furthermore, filtration of fine solid particles is important in many industrial processes, for example in the removal of particulate matter from exhaust gases. In such systems, the events governing the overall performance of the device are occurring on micro- or nano-scales. It is not yet well established how particle motion and filtration are affected by non-isothermal conditions at these small spatial scales. In addition, when the particle size is comparable to the mean free path of the gas, rarefaction effects become important.

In the derivation of closure laws for use in numerical simulations of industrial units, direct numerical simulations of the events on the microscale are important. The primary interest here is thus to perform numerical investigations of the flow phenomena on the scale of the particles using a direct numerical simulation (DNS) approach. We use the term "multiphase direct numerical simulations (DNS)" to denote numerical simulations of multiphase flows where one resolves the temporal and spatial scales relevant to the fluid dynamics. In the present work, we present a comprehensive multiphase DNS framework in which all of the aforementioned physics can be included simultaneously.

With such DNS techniques, the Navier-Stokes equations are solved directly, together with a method for taking the presence of particles into account. Some of the most common multiphase DNS methods include the Volume of Fluid (VOF) method (Hirt and Nichols 1981), the front tracking method (Tryggvason et al. 2001), the immersed boundary methods (Peskin 2002; Mittal and Iaccarino 2005; Uhlmann 2005; Kim and Choi 2006; Mittal et al. 2008), and Lagrange multiplier/fictitious domain methods (Glowinski et al. 1999; Glowinski et al. 2001; Sharma and Patankar 2005; Apte et al. 2009; Apte and Finn 2010). In addition, there exist methods where the fluid flow near an immersed object is locally matched to the corresponding Stokes flow solution

(Zhang and Prosperetti 2005). There are also several level-set methods available for capturing the position and evolving topology of fluid-fluid interfaces (e.g. Lahey 2009). Finally, recent progress in the development of the macro-scale pseudo-particle method (MaPPM) has enabled DNS of very large dispersed multiphase systems to be carried out on GPU-based HPC systems (Ma et al. 2006; Ma et al. 2009; Xiong et al. 2010).

Although direct numerical simulations of multiphase systems with simultaneous heat transfer and solid particles motion is still an emerging field, a number of methods have already been presented in the literature. Of these, the distributed Lagrange multiplier/fictitious domain method (Yu et al. 2006; Wachs 2011) and the immersed-boundary method (Feng and Michaelides 2009) have received most attention. Recently, a method in which the fluid-solid coupling is accomplished at the level of the discrete momentum and thermal energy balance equations has also been proposed (Deen et al. 2012).

As previously stated, simultaneous momentum, heat and mass transfer is common in industrial gas-solid systems. Moreover, the particles might be solid or sometimes droplets, or even solid structures with condensed material over the surface. For applications involving fluid-like particles, the VOF multiphase model is considered an appropriate framework (Lakehal et al. 2002). Furthermore, among multiphase DNS techniques, the VOF model is relatively simple to implement and computationally efficient since it avoids explicit computation of the hydrodynamic force and torque on the particles (Jakobsen 2008).

In the current work, we propose a VOF technique to handle solid particles motion coupled with heat transfer effects. This method resolves both the temperature field of the carrier phase and that inside the particles. No restrictions on the particle Biot number or the variations of the fluid properties are introduced in the derivation, although the Boussinesq model is employed for validation purposes. The model is valid for Knudsen numbers of up to unity in unbounded flow. We herein present numerical results that constitute a validation of the method, as well as a discussion about situations in which the currently proposed method represents a competitive choice for performing numerical investigations of dispersed multiphase systems.

2. MODELLING AND NUMERICS

A shared set of balance equations is used for the continuous phase and the dispersed phases. These dispersed phases can be solid particles and/or fluid particles (i.e. droplets or bubbles). For a system of N_P solid particles, the volume fraction of the carrier fluid in a computational cell is denoted γ_f and the volume fraction of the i:th particle is designated $\gamma_{p,i}$. To avoid inadvertent particle coalescence, particles that touch each other must be interpreted as separate phases and hence exist in different volume fraction fields. The subscript j in the variable $\gamma_{p,i,j}$ thus represents the volume fraction of the i:th particle present in the j:th volume fraction field. The total number of volume fraction fields employed is denoted N_{VF}, and the sum of all volume fractions in a computational cell is unity:

$$\gamma_f + \sum_{j=1}^{N_{VF}}\left(\sum_{i=1}^{N_P}\gamma_{p,i,j}\right) = 1 \tag{1}$$

The herein proposed method puts no restriction on N_P, and we drop the particle identity subscript and summation for typographical reasons from this point.

The velocity field is determined from the shared continuity and momentum equations, assuming that the flow is incompressible and that the velocity of the two phases is continuous across the interface:

$$\nabla \cdot u = 0 \tag{2}$$

$$\rho\left(\frac{\partial u}{\partial t} + u \cdot \nabla u\right) = -\nabla P + \nabla \cdot [\mu(\nabla u + (\nabla u)^T)] + \{[1 - \beta(T - T_0)]\gamma_f \rho_{f,0} + \gamma_p \rho_p\}g + F_\sigma \tag{3}$$

As may be seen from the gravitational term in equation (3), the Boussinesq (1903) model is employed to describe the variation of the buoyancy force with temperature.

The shared density and viscosity in equation (3) are determined locally using:

$$\rho = \rho_f \left(\gamma_f + \gamma_p \rho_{ptf} \right) \tag{4}$$

$$\mu = \mu_f \left(\gamma_f + \gamma_p \mu_{ptf} \right) \tag{5}$$

where ρ_{ptf} and μ_{ptf} indicate the particle-to-fluid ratio of densities and viscosities, respectively.

The effects of rarefication can be taken into account by exchanging the particle density for an adjusted density ρ^* (Ström et al., 2011):

$$\rho^* = \rho_p \left(1 + Kn_p \left[1.155 + 0.471\, exp \left(-\frac{0.596}{Kn_p} \right) \right] \right) \tag{6}$$

Here, Kn_p is the particle Knudsen number based on the particle radius. In the continuum limit, Kn_p goes to zero and ρ^* becomes equal to the particle density ρ_p, meaning that the conventional continuum representation of the simulation framework is recovered.

The presence of the particles is monitored by solving N_{VF} continuity equations for the particulate phase:

$$\frac{\partial \gamma_{p,i,j}}{\partial t} + \nabla \cdot \left(\gamma_{p,i,j} u \right) = 0 \tag{7}$$

Note that the formulation in equation (7) inherently obeys the boundary conditions of matching velocities, pressures and temperatures of the fluid and solid regions, as well as matching momentum and heat fluxes. It is the enforcement of these boundary conditions that constitute the core of the fictitious-domain/immersed-boundary methods. In contrast, the challenge in the VOF framework lies in making sure that the particles behave as solid, rigid particles.

The VOF method was originally proposed by Hirt and Nichols (1981) for simulations of gas-liquid and liquid-liquid systems. Using VOF for handling also solid particles motion requires some additional considerations:

1) The velocity boundary condition at the interface between the solid particle and the fluid should replicate that of no slip. Therefore, μ_{ptf} in equation (5) should approach infinity in the regions occupied by solid particles. In practice, a sufficiently high numerical value is acceptable (Ström et al. 2011).

2) A unidirectional velocity field is enforced inside each solid particle by updating the shared velocity field at the end of each time step according to:

$$u_c^{new} = \gamma_f u_c^{old} + \sum_{j=1}^{N_{VF}} \left(\sum_{i=1}^{N_P} \gamma_{p,i,j} \overline{u}_{p,i} \right) \tag{8}$$

where the velocity of the i:th particle is obtained from:

$$\overline{u}_{p,i} = \frac{\sum_c \gamma_{p,i,c} \rho_p V_c u_c^{old}}{\sum_c \gamma_{p,i,c} \rho_p V_c} \tag{9}$$

and u_c^{old} is one of the velocity components in cell index c before the update, V is the volume of a computational cell and the summation is carried out over all cells of the computational domain. The weighting of the old and new velocity fields conserves momentum, and the computational cost of the update loop is insignificant compared with the cost of performing a sub-iteration within a time step.

3) The term F_σ in equation (3) represents a force designed to ensure that a solid particle retains its spherical shape (Brackbill et al. 1992; Ström et al. 2011):

$$F_\sigma = \frac{\sigma\rho(\nabla\cdot\hat{n})\nabla\gamma}{\frac{1}{2}\left(\rho_f + \rho_p\right)} \tag{10}$$

Here, $\hat{n}$ is the unit normal to the fluid-particle surface. The value of σ, which may be interpreted as a fictitious surface tension between the solid particle and the carrier fluid, is updated globally in every time step using:

$$\sigma = \mu U / Ca_{max} \tag{11}$$

so that the restriction that the maximal Capillary number for the solid particle remains below 0.05 is always valid.

In the interior of the computational domain, the unit normal is calculated locally as:

$$\hat{n} = \frac{n}{|n|} = \frac{\nabla\gamma_p}{\left|\nabla\gamma_p\right|} \tag{12}$$

To maintain the spherical shape of the particle also in the case where the particle enters the cell layer next to the wall, the unit normal within these cells is set to approach the wall-normal unit vector. Numerically, this is achieved by modeling the unit wall normal in this cell layer as:

$$\hat{n} = \hat{e}_n cos\theta + \hat{e}_t sin\theta \tag{13}$$

while using a value of the numerical parameter θ that is close to 180°. In equation (13), $\hat{e}_n$ represents the normal unit vector and $\hat{e}_t$ the tangential one. As the expression for F_σ is based on the continuum surface force model (Brackbill et al. 1992), the choice of θ may be physically interpreted as a particle-wall contact angle. Consequently, it implicitly determines the degree of particle deformation allowed upon contact or collision with a wall.

It becomes important that each solid particle exists in a different volume fraction field if two or more particles come in close proximity of each other. Otherwise, particle coalescence could inadvertently occur. To guarantee that solid particles in close proximity of each other always exist in separate volume fraction fields, a control algorithm is implemented that moves the particles between different fields as required by the current state of the solution. The procedure followed by the volume fraction field control algorithm thus becomes:

1)   Update the current particle locations.
2)   Identify possible future collision partners.
3)   Move any identified solid particle within another solid particle's close proximity to another volume fraction field.

The temperature field is obtained by solving an energy balance equation:

$$\frac{\partial}{\partial t}\left(\gamma_p\rho_p E_p + \gamma_f\rho_f E_f\right) + \nabla\cdot\left[u\left(\gamma_p\rho_p E_p + \gamma_f\rho_f E_f + P + \frac{\rho u^2}{2}\right)\right] = \nabla\cdot\left(k\nabla T\right) \tag{14}$$

where

$$E_f = \int_{T_{ref}}^{T} c_{p,f}\, dT \tag{15}$$

and

$$E_p = \int_{T_{ref}}^{T} c_{p,p}\, dT \tag{16}$$

In the same way as with the pressure and velocity, the continuous and dispersed phases share a single temperature field. The local value of the thermal conductivity is determined using:

$$k = k_f \left(\gamma_f + \gamma_p k_{ptf} \right) \tag{17}$$

The effects of rarefaction on the heat transfer are taken into account by exchanging the particle heat capacity for an adjusted heat capacity (Ström and Sasic, 2013a):

$$c_p^* = \frac{c_{p,p} \left(1 + \frac{15}{4} \alpha^{-1} Kn_p \right)}{1 + Kn_p \left[1.155 + 0.471 exp \left(-\frac{0.596}{Kn_p} \right) \right]} \tag{18}$$

Equations (2), (3) and (14) are discretized on a co-located grid using the QUICK scheme for the convection terms and a second-order accurate central-differencing scheme for the diffusion terms. The pressure-velocity coupling algorithm is PISO, and PRESTO! is used as the pressure interpolation scheme. Equation (7) is discretized using the CICSAM scheme (Ubbink 1997).

The temporal discretization of all balance equations is first-order implicit, with the exception of equation (7). The solution of the latter equation is advanced in time using explicit time stepping and a time step that is limited by the constraint that the global CFL number must remain below 0.25. A small CFL number, when used with explicit time stepping and a robust spatial discretization scheme with an upwind character, counteracts numerical diffusion that could otherwise lead to smearing of the interface profile (Darwish and Moukalled 2006). It also assists in avoiding convergence problems, at the expense of having to take a larger number of time steps in the update of equation (7). To maintain computational efficiency, the update of equation (7) is therefore performed only once at the beginning of every fluid flow time step, so that the volume fraction fields are frozen during the iterative solution of the continuity, momentum and energy balance equations. It was also confirmed that the small CFL numbers employed imply that any effects of this procedure on the number of sub-iterations needed within a time step are very small.

3. RESULTS AND DISCUSSION

In this section, the predictions of the current numerical method are compared to the available data for a number of important validation cases: solid particles motion during isothermal conditions in the presence of walls and other particles, natural convection around a stationary particle, and solid particles motion accompanied with heat transfer effects. Finally, it is shown how the method can be applied to investigate the simultaneous effects of heat transfer and rarefaction on the motion of a solid catalyst particle in an enclosure and the outcome of the interaction of a solid particle and a microbubble in a flotation cell.

The choice of variables by which to non-dimensionalize the results is not entirely straightforward (Wachs 2011). Here, we choose the approach of Yu et al. (2002) and make the velocity dimensionless by a characteristic velocity $U = d_p^2 \left(\rho_p - \rho_f \right) g / 16 \mu$ that is representative of the terminal velocity, whereas the position and time are scaled by the particle diameter and the characteristic time scale $t = d_p / U$ respectively. The drag force is made dimensionless by scaling with the Stokes drag, $F = 3\pi\mu d_p U$.

Since the proposed method is developed for investigations of systems of many particles in wall-bounded domains, it is of great importance to verify that the method is capable of predicting the interaction of a particle with a wall and other particles. In the presence of surfaces, e.g. walls or other particles, the drag force on a particle increases in comparison to the situation when the particle is isolated in an unbounded domain. The correct drag force can, under such circumstances, be obtained by multiplying the Stokes drag with a drag modification function, λ.

In Figure 1, a particle is settling towards a plane at its terminal velocity in the carrier fluid. The fluid properties are chosen so that the particle motion remains within the Stokes flow regime at all times. In this situation, the drag modification function is only a function of the distance between the plane and the particle. Brenner (1961) derived analytically λ for a sphere moving towards either a no-

slip plane or a free-slip plane. A no-slip plane would represent either a wall or the surface of a (large) solid particle, whereas a free-slip plane represents a free surface or the surface of a (large) bubble.

When we compare the Brenner (1961) results to the drag modification observed in three-dimensional numerical simulations of the identical problem using the proposed method, it is found that the current method is in very good agreement with the Brenner solution. In Figure 1, the particle-plane distance is taken from the plane surface to the particle center and is normalized by the particle radius (i.e. a distance equal to unity indicates that the surfaces are in contact).

The drag modification function for a particle approaching another (identical) particle was measured experimentally by Adamczyk et al. (1983). In Figure 2, the predicted drag modification
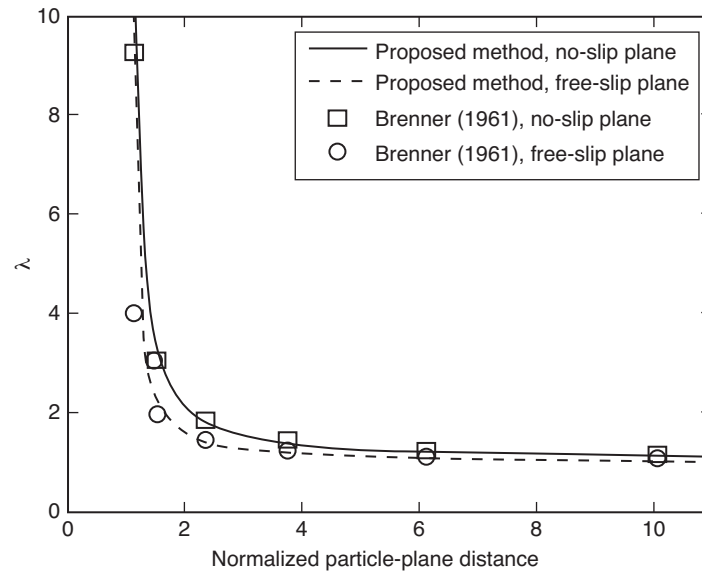

Figure 1: Drag modification function (λ) plotted versus the particle-plane distance. The particle is approaching a plane where either a no-slip or a free-slip boundary condition is imposed for fluid flow.
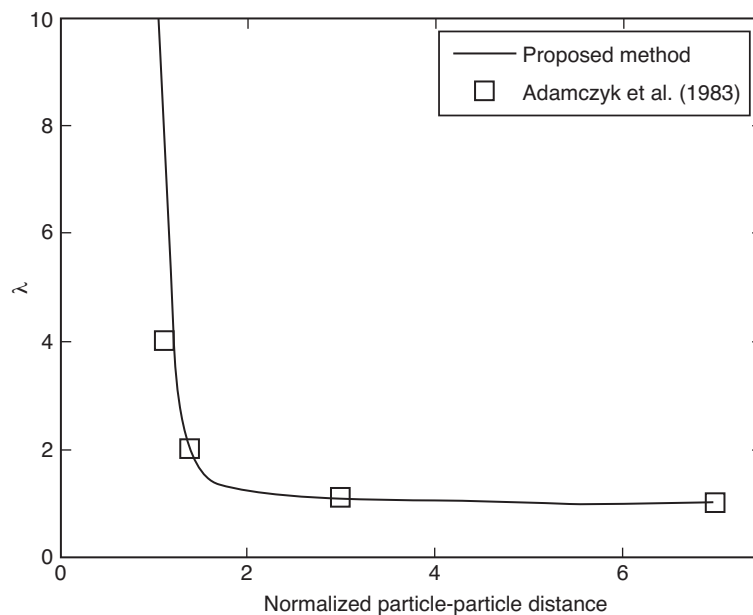

Figure 2: Drag modification function (λ) plotted versus the particle-particle distance. The particle-particle distance is taken from the stationary particle surface to the moving particle center and is normalized by the particle radius (i.e. a distance equal to unity indicates that the particle surfaces are in contact).

from the method proposed in this paper is compared to their data. The governing parameters for this problem are the particle-particle separation and the particle-particle size ratio (the latter being unity in our comparison). Again, the particle motion remains within the Stokes flow regime throughout the interaction. As with the approach towards a plane, the agreement observed is very good. The slight disagreement at the smallest particle-particle distance can be explained by the decision not to dynamically refine the mesh in the region between the two particles.

The next validation simulation treats natural convection around a stationary particle. This is an example of heat transfer-induced fluid motion that becomes of great importance when the particle motion takes place simultaneously as the particle-fluid heat transfer, and when the two phenomena have a significant impact on each other.

This case of a circular cylinder placed eccentrically in a square enclosure is used for validation of the current model against the numerical results of several works in which different multiphase DNS methods were used to handle the same problem and whose results all agree well (Demirdzic et al. 1992; Pacheco et al. 2005; Yu et al. 2006; Feng and Michaelides 2009).

The computational domain is a two-dimensional square box ($2.5d_p \times 2.5d_p$) and the particle is represented by a circular cylinder placed eccentrically ($0.25d_p$ above the center) in the enclosure. The cylinder is stationary and at a constant temperature that is higher than that of the surrounding fluid. The vertical walls are kept at the initial temperature of the fluid, whereas the top and bottom walls are adiabatic. The steady-state solution for the natural convection inside the enclosure is obtained and compared to the aforementioned previous studies. The governing dimensionless numbers are Pr = 10 and Gr = 10^5. The result is shown in Figure 3, where the iso-contours of temperature are depicted. The isotherms obtained by the proposed method agree very well with the results of Feng and Michaelides (2009), and hence also with the other previous investigations (Demirdzic et al. 1992; Pacheco et al. 2005; Yu et al. 2006). We regard this as a confirmation that the energy balance equation is correctly implemented within the current framework.

Next, we consider the settling of a particle in an adiabatic two-dimensional enclosure ($8d_p \times 16d_p$) under the influence of gravity and heat transfer effects. The particle and the surrounding fluid are initially of the same temperature, and the particle is positioned in the middle of the enclosure. There is however a uniform heat source inside the particle that increases the temperature of the particle (and eventually also its surroundings). The evolution of the particle velocity in the vertical direction is monitored as a function of time.

The governing dimensionless parameters for these cases are given in Table 1. The results are shown in Figure 4, together with the results obtained by Yu et al. (2006), Feng and
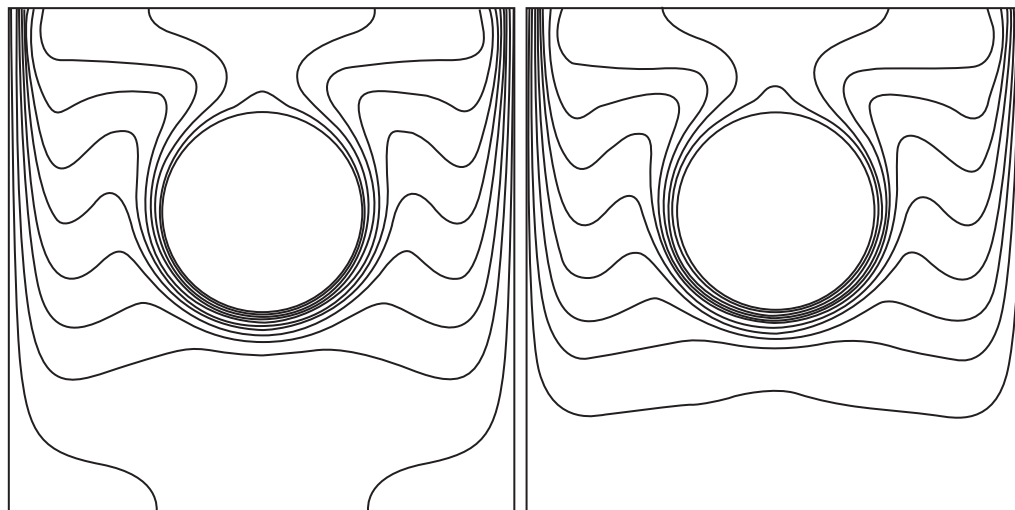

Figure 3: A hot cylinder placed eccentrically in a square enclosure. Left: Current work.Right: Feng and Michaelides (2009). The contour levels represent 0.1 units of normalized temperature on the interval 0.05-0.95 (cold = black, hot = white). The isotherms agree well, the only difference being the 0.05 contour, farthest away from the cylinder.

Table 1. The governing dimensionless parameters used in the validation simulations.

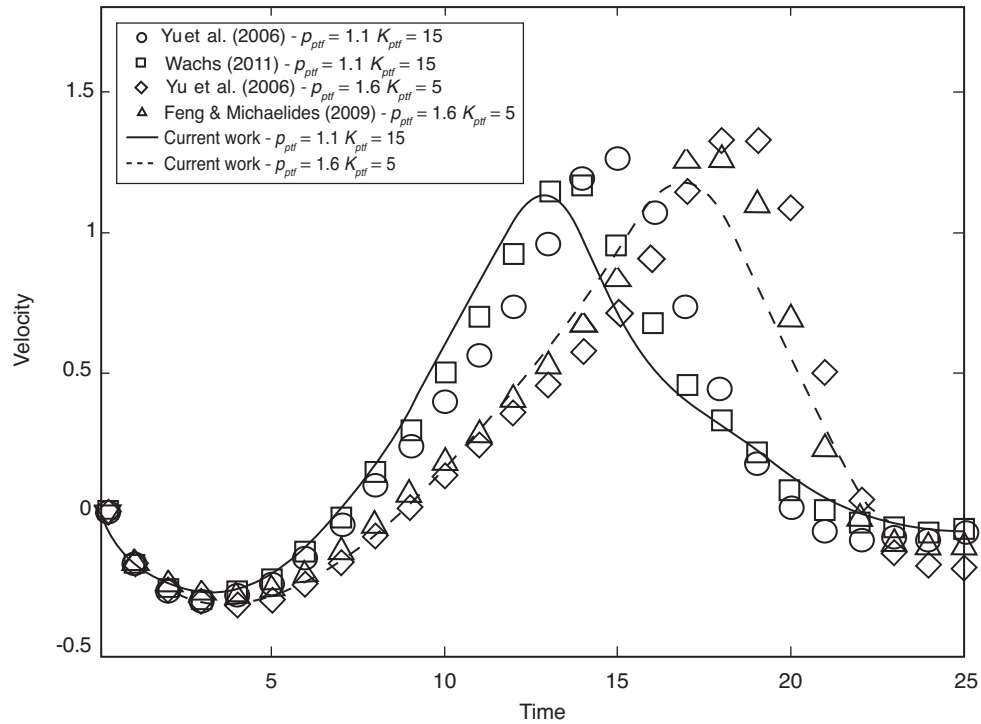| Parameter	$Re_{p,T}$	ρ_{ptf}	k_{ptf}	$c_{p,ptf}$	Gr	β_{ptf}	Pr	Kn_p
Value	40	1.1 or 1.6	5 or 15	1	1000	0	0.7	0

Figure 4: Settling particle with an internal heat source in continuum flow. Validation of the current framework to the works of Yu et al. (2006), Feng and Michaelides (2009) and Wachs (2011).

Michaelides (2009) and Wachs (2011) for the same problem. The simulations predict that the particle initially falls towards the bottom of the enclosure. However, the heating of the boundary layer around the particle eventually gives rise to a buoyancy force that first counterbalances and then overcomes the gravitational acceleration of the particle. The particle therefore starts to move upwards, until the effects of the upper wall become apparent. The particle motion is then slowed down because of the aerodynamic resistance, and because of the geometry that restricts and weakens the natural convection currents that carry the particle upwards. The current model is in good agreement with all of the three previous works. The minor differences observed are within the bounds expected due to the different choices of coupling methods and discretization schemes, given the very sensitive thermo-mechanical coupling of the system (Wachs 2011; Ström and Sasic, 2013b).

The case with a particle with an internal heat source in an enclosure can be thought to represent that of a catalyst particle, catalysing an exothermic chemical reaction, inside a pore or a cavity. In a real application, it is therefore likely that the particle will be very small; it might in fact even be significantly smaller than the mean free path of the surrounding fluid. In such rarefied flow, the particle motion history is similar but delayed (slower) compared to the continuum case. Firstly, the rarefied fluid surrounding the particle cannot resist the initial particle acceleration due to gravity as in the continuum case. In a rarefied case, the particle therefore falls farther than in a continuum case. Secondly, the impeded heat transfer from the particle to the fluid delays the growth of the buoyancy force. Consequently, the particle attains a larger downward velocity before changing direction with increasing Kn_p.

Although the main effect of the rarefication is to delay the growth of a sufficiently large buoyancy force for the particle downward acceleration to be fully outweighed, the net result is not limited to merely slowing down of the same process that occurs in the continuum regime. Since thermal levitation and/or lifting up of the particle can only occur if there is sufficient space available for the natural convection streams underneath the particle to fully develop (Wachs 2011), the delay observed in the rarefied regime may actually prevent the upward motion of the particle altogether by shifting the heating-up of the fluid to a later point in time when the space underneath the particle may have become too small. This phenomenon is illustrated by the particle vertical trajectories plotted in Figure 5 for $\rho_{ptf} = 20$, where the particle eventually moves upward in the continuum case but falls to the bottom of the enclosure for ($Kn_p = 0.5$, $\alpha_t = 1$).

Next, we demonstrate the capability of the proposed method to handle rigid and deformable particles (e.g. bubbles) simultaneously, by investigating the interaction of a settling solid particle and a rising bubble. The interaction is illustrated in Figure 6 for a case where the two entities are initially moving directly towards each other in the vertical direction, as the bubble is rising and the particle is settling with their terminal velocities. The tendency to bubble deformation is varied in this numerical experiment by employing two different values of the surface tension between air and water. In practice, such a change could be achieved through an addition of surfactants to the water.

When the contact between a particle and a bubble is likely to occur, the particle density plays a significant role. The interaction between a spherical bubble and a light particle is illustrated in Figure 6a, and it is expected that there could be a contact between them. In fact, the direction of motion of the light particle is changed before touching the surface of the bubble, and it is carried upwards by the bubble. However, as the pair moves together towards the surface, the distance between them decreases at all times, which might result in a contact before reaching the free surface of the suspension. A similar behaviour may be observed for the light particle approaching the deforming bubble (see Figure 6b).

In contrast, a heavy particle becomes entirely surrounded by the approaching deformed bubble, as shown in Figure 6c. After that, the particle passes through the bubble. In other words, the downward movement of a heavy particle leads to a complete distortion of the deforming bubble. Whereas an addition of surfactants might reduce the risk of a light solid particle bouncing off or
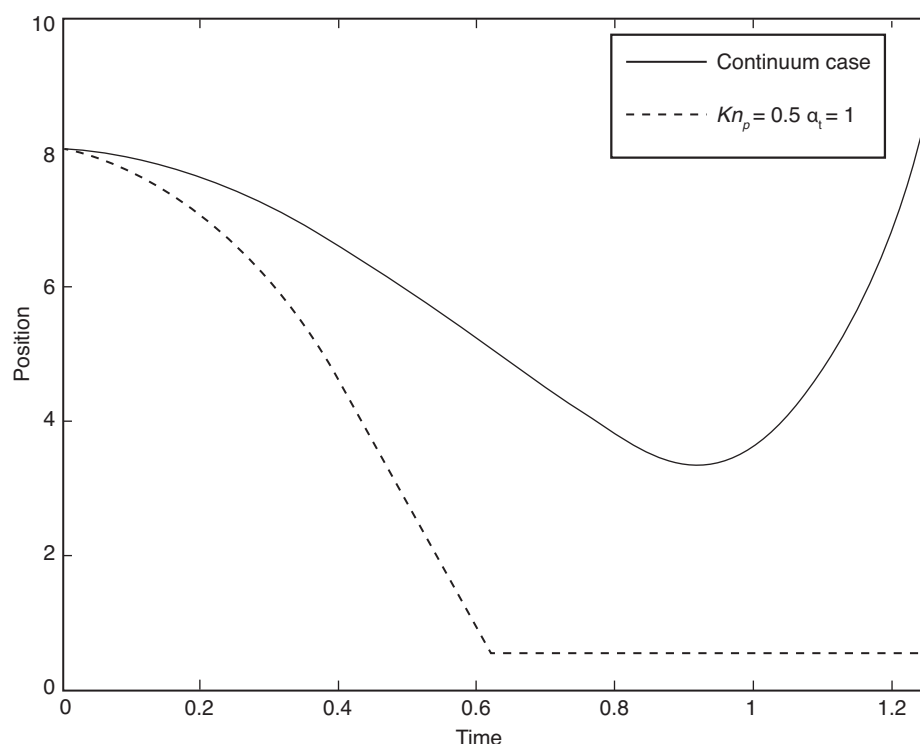

Figure 5: Particle vertical position versus time in continuum and rarefied flow ($\rho_{ptf} = 20$).
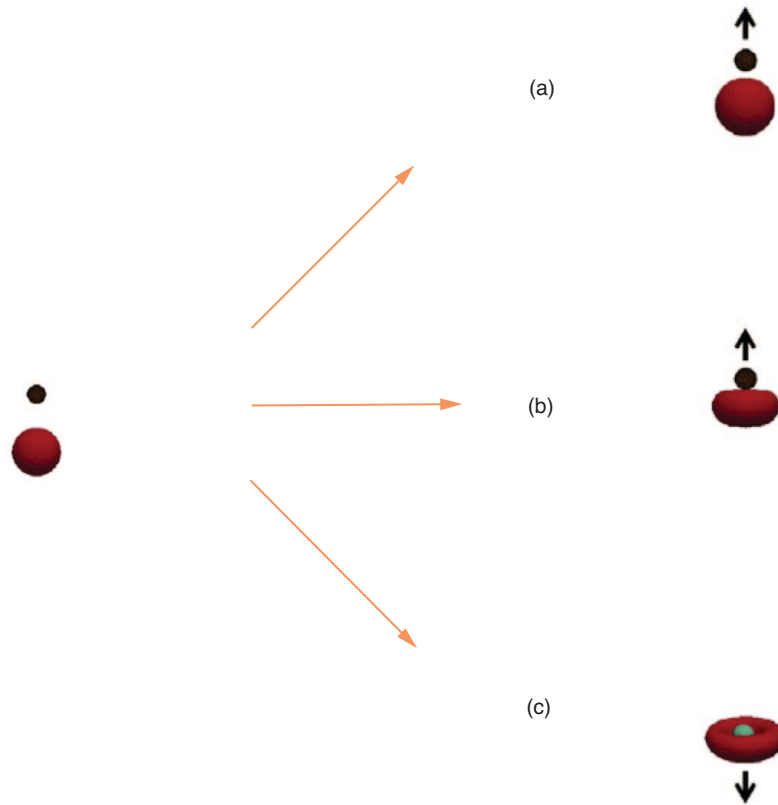
Figure 6: Snapshots of bubble-particle encounters: (a) a light particle and a spherical bubble, (b) a light particle and a deforming bubble, and (c) a heavy particle and a deforming bubble.

sliding over a spherical bubble (by allowing the bubble to deform slightly), it is found that a heavier particle could instead destroy the deforming bubble.

In a more general particle-bubble interaction, the approach of the two entities may not be along the axis of symmetry. The limiting case where particle-bubble close contact may still occur hydrodynamically in spite of an initial separation in the horizontal plane is denoted the grazing radius configuration. The difference in behavior between a spherical and a deformed bubble in this type of interaction is exemplified in Figure 7. Here, the grazing radius configuration corresponds to an initial horizontal separation equal to approximately 65% of the bubble radius (Sasic et al., 2014). The interaction of two different types of bubbles (one spherical and one deforming) with a light particle is studied. In both cases, the interaction with the bubble causes the particle to attain a horizontal velocity away from the bubble as the two entities are coming close to each other. Even so, the particle collides with the spherical bubble, as shown in Figure 7a. However, there will be no collision when the bubble deforms (Figure 7b). This further strengthens the previous conclusion that the probability of formation of bubble–particle agglomerates is decreased for bubbles that can easily deform.

Finally, we study the performance of the suggested modelling framework for a case in which the number of particles is significantly increased. For this purpose, a two-dimensional enclosure containing 1024 particles is considered. The size of the enclosure is $65d_p \times 65d_p$ and the computational mesh contains 1.69 million cells (i.e. 20 cells per particle diameter). The governing dimensionless parameters are $(\rho_{ptf}, k_{ptf}) = (1.6, 5)$. Figure 8 shows a snapshot from such a simulation after it has evolved for 22 units of dimensionless time. It is clear from the close-up view that the method is capable of resolving the internal temperature gradients inside the particles. Furthermore, the particles are significantly affecting each other's boundary layers in terms of both momentum and energy transfer. The current method is capable of handling this situation without
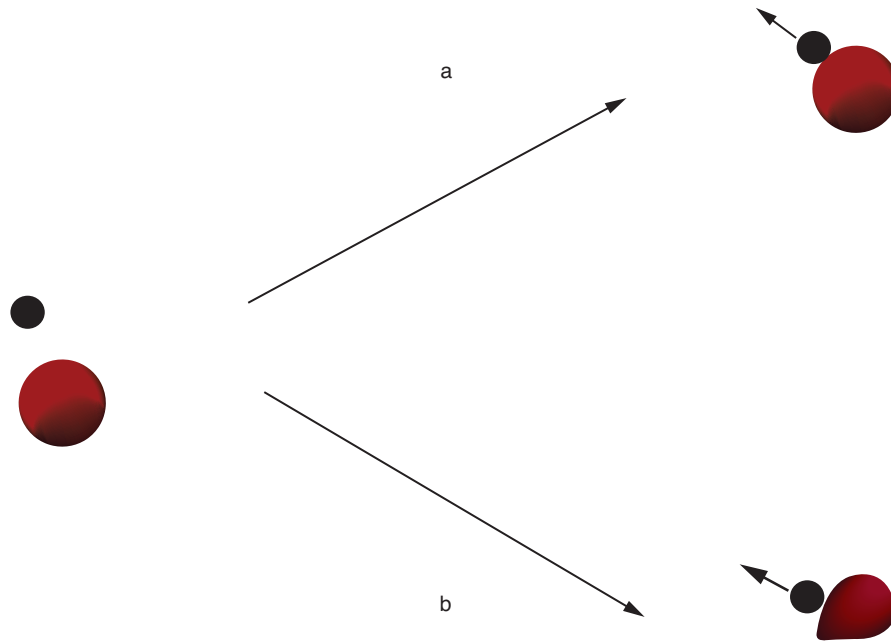
Figure 7: Snapshots at different times for a grazing radius configuration, where a light
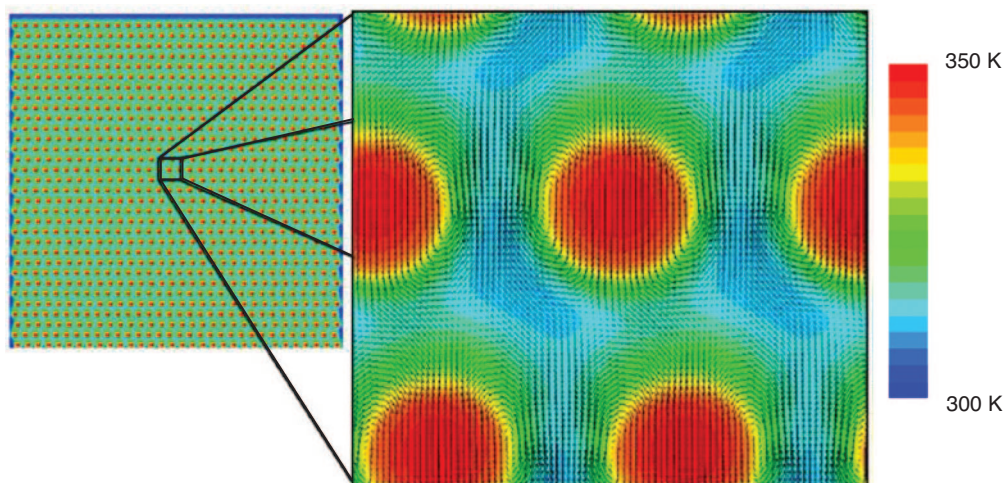particle interacts with (a) a spherical or (b) a deforming bubble.

Figure 8: A snapshot from a simulation with 1024 particles (ρ_{ptf} = 1.6, k_{ptf} = 5) moving in
a 2D square enclosure (taken at t = 22). Velocity vectors (black) are
overlaid onto a contour plot of the temperature field.

difficulties. In the future, the method could therefore be applied to study particle clustering in non-isothermal dispersed multiphase flows (cf. Ma et al. 2009; Agrawal et al. 2013).

4. CONCLUSIONS

In this paper we present a multiphase DNS method that can be applied to resolve the motion of solid and deformable particles with heat transfer effects in continuum or rarefied flow. The method is based on solving a shared set of momentum and energy balance equations for the carrier phase and the particulate phase. Additional numerical procedures are applied to ensure that the solid particles behave as rigid entities. The proposed method is validated against numerical data available in the literature (Brenner 1961; Adamczyk et al. 1983; Yu et al. 2006; Feng and Michaelides 2009; Wachs 2011; Ström 2011) and very good agreement is found overall.

The current method is inherently capable of handling liquid particles co-existing with solid particles, and is thus well suited to handle challenging multiphase systems, such as diesel spray combustion with soot formation, spray drying with particle nucleation, etc.

ACKNOWLEDGEMENTS

NOMENCLATURE

Ca	Capillary number (–)
c_p	heat capacity (J kg^{-1} K^{-1})
d	diameter (m)
E	energy per mass (J/kg)
$\hat{e}$	unit normal (–)
F	force (N)
g	gravitational constant (m s^{-2})
Gr	Grashof number (–)
k	thermal conductivity (W m^{-1} K^{-1})
Kn	Knudsen number (–)
N	number (–)
$\hat{n}$	unit normal (–)
P	pressure (N m^{-2})
Pr	Prandtl number (–)
Re	Reynolds number
T	temperature (K)
t	time (s)
V	volume (m^3)
u	velocity (m s^{-1})
U	characteristic velocity (m s^{-1})

Greek letters

α_t	thermal accommodation coefficient (–)
β	thermal expansion coefficient (K^{-1})
γ	volume fraction (–)
λ	drag modification function (–)
θ	numerical parameter (°)
σ	surface tension (N m)
ρ	density (kg m^{-3})
μ	viscosity (Pa s)

Subscripts

c	cell index
f	fluid
i, j	index
max	max
new	new
old	old
p	particle
P	particles
ptf	particle-to-fluid
r	relative

Superscripts

*	adjusted

REFERENCES

[1] Z. Adamczyk, M. Adamczyk, and T. G. M. van de Ven, Resistance coefficient of a solid sphere approaching plane and curved boundaries, *J. Colloid Interface Sci.*, 96, 1983, 204–213.

[2] K. Agrawal, W. Holloway, C. C. Milioli, F. E. Milioli and S. Sundaresan, Filtered models for scalar transport in gas-particle flows, *Chem. Eng. Sci.*, 95, 2013, 291–300.

[3] S. V. Apte, M. Martin, and N. A. Patankar, A numerical method for fully resolved simulations (FRS) of rigid particle-flow interactions in complex flows, *J. Comput. Phys.*, 228, 2009, 2712–2738.

[4] S. V. Apte, and J. Finn, A variable-density fictitiuos-domain method for fully resolved simulation of high-density ratio fluid-particle systems, *Proc. 7th Int. Conf. Multiphase Flow (ICMF-2010), Tampa, FL, USA*, 2010.

[5] J. Boussinesq, *Théorieanalytique de la chaleur*, Gathier-Villars, Paris, 1903.

[6] H. Brenner, The slow motion of a sphere through a viscous fluid towards a plane surface, *Chem. Eng. Sci.*, 16, 1961, 242–251.

[7] M. Darwish, and F. Moukalled, Convective schemes for capturing interfaces of free-surface flows on unstructured grids, *Num. Heat Transfer B*, 49, 2006, 19–42.

[8] Z.-G. Feng, and E. E. Michaelides, Heat transfer in particulate flows with Direct Numerical Simulation (DNS), *Int. J. Heat Mass Transfer*, 52, 2009, 777–786.

[9] R. Glowinski, T.-W. Pan, T. I. Hesla, and D. D. Joseph, A distributed Lagrange multiplier/fictitiuos domain method for particulate flows, *Int. J. Multiphase Flow*, 25, 1999, 755–794.

[10] R. Glowinski, T.-W. Pan, T. I. Hesla, D. D. Joseph, and J. Periaux, A fictitious domain approach to the direct numerical simulation of incompressible viscous flow past moving rigid bodies - application to particulate flow, *J. Comput. Phys.*, 169, 2001, 363–426.

[11] C. W. Hirt, and B. D. Nichols, Volume of fluid (VOF) method for the dynamics of free boundaries, *J. Comput. Phys.*, 39, 1981, 201–225.

[12] N. G. Deen, S. H. L. Kriebitzsch, M. A. van der Hoef, and J. A. M. Kuipers, Direct numerical simulation of flow and heat transfer in dense fluid-particle systems, *Chem. Eng. Sci.*, 81, 2012, 329–344.

[13] I. Demirdzic, Z. Lilek, and M. Peric, Fluid flow and heat transfer test problems for non-orthogonal grids: bench-mark solutions, *Int. J. Numer. Meth. Fluids*, 15, 1992, 329–354.

[14] H. A. Jakobsen, *Chemical Reactor Modeling. Multiphase Reactive Flows*, Springer-Verlag, Berlin Heidelberg, 2008.

[15] D. Kim, and H. Choi, Immersed boundary method for flow around an arbitrarily moving body, *J. Comput. Phys.*, 212, 2006, 662–680.

[16] R. T. Lahey Jr., On the direct numerical simulation of two-phase flows, *Nucl. Eng. Des.*, 239, 2009, 867–879.

[17] D. Lakehal, M. Meier, and M. Fulgosi, Interface tracking towards the direct simulation of heat and mass transfer in multiphase flows, *Int. J. Heat Fluid Flow*, 23, 2002, 242–257.

[18] J. Ma, W. Ge, X. Wang, J. Wang and J. Li, High-resolution simulation of gas-solid suspension using macro-scale particle methods, *Chem. Eng. Sci.*, 61, 2006, 7096–7106.

[19] J. Ma, W. Ge, Q. Xiong, J. Wang and J. Li, Direct numerical simulation of particle clustering in gas-solid flow with a macro-scale particle method, *Chem. Eng. Sci.*, 64, 2009, 43–51.

[20] R. Mittal, and G. Iaccarino, Immersed boundary methods, *Ann. Rev. Fluid Mech.*, 37, 2005, 239-261.

[21] R. Mittal, H. Dong, M. Bozkurttas, F. M. Najjar, A. Vargas, and A. von Loebbecke, A versatile sharp interface immersed boundary method for incompressible flows with complex boundaries, *J. Comput. Phys.*, 227, 2008, 4825–4852.

[22] J. R. Pacheco, A. Pacheco-Vega, T. Rodic, and R. E. Peck, Numerical simulations of heat transfer and fluid problems using an immersed-boundary finite-volume method on non-staggered grids, *Numer. Heat Transfer B*, 48, 2005, 1–24.

[23] C. S. Peskin, The immersed boundary method, *Acta Numer.*, 11, 2002, 479–517.

[24] S. Sasic, E. K. Sibaki, and H. Ström, Direct numerical simulations of a hydrodynamic interaction between settling particles and rising microbubbles, *Eur. J. Mech. B-Fluid*, 43, 2014, 65–75.

[25] N. Sharma, and N. A. Patankar, A fast computation technique for the direct simulation of rigid particulate flows, *J. Comput. Phys.*, 205, 2005, 439–457.

[26] H. Ström, S. Sasic, and B. Andersson, A novel multiphase DNS approach for handling solid particles in a rarefied gas, *Int. J. Multiphase Flow*, 37, 2011, 906–918.

[27]   H. Ström, and S. Sasic, Heat transfer effects on particle motion under rarefied conditions, *Int. J. Heat Fluid Flow*, 43, 2013a, 277–284.

[28]   H. Ström, and S. Sasic, A multiphase DNS approach for handling solid particles motion with heat transfer, *Int. J. Multiphase Flow*, 53, 2013b, 75–87.

[29]   G. Tryggvason, B. Bunner, A. Esmaeeli, D. Juric, N. Al-Rawahi, W. Tauber, J. Han, S. Nas, and Y.-J. Jan, A front-tracking method for the computations of multiphase flow, *J. Comput. Phys.*, 169, 2001, 708–759.

[30]   O. Ubbink, *Numerical prediction of two fluid systems with sharp interfaces*, PhD thesis, Imperial College of Science, Technology & Medicine, London, 1997.

[31]   M. Uhlmann, An immersed boundary method with direct forcing for the simulation of particulate flows, *J. Comput. Phys.*, 209, 2005, 448–476.

[32]   Z. Yu, X. Shao, and A. Wachs, A fictitious domain method for particulate flows with heat transfer, *J. Comput. Phys.*, 217, 2006, 424–452.

[33]   Z. Yu, N. Phan-Thien, Y. Fan, and R. I. Tanner, Viscoelastic mobility problem of a system of particles, *J. Non-Newtonian Fluid Mech.*, 104, 2002, 87–124.

[34]   A. Wachs, Rising of 3D catalyst particles in a natural convection dominated flow by a parallel DNS method, *Computers Chem. Eng.*, 35, 2011, 2169–2185.

[35]   Q. Xiong, B. Li, F. Chen, J. Ma, W. Ge and J. Li, Direct numerical simulation of sub-grid structures in gas-solid flow – GPU implementation of macro-scale pseudo-particle modeling, *Chem. Eng. Sci.*, 65, 2010, 5356–5365.

[36]   Z. Zhang, and A. Prosperetti, A second-order method for three-dimensional particle simulation, *J. Comput. Phys.*, 210, 2005, 292–324.